Journal of Applied Polymer Science

# Outdoor Weathering of Polyamide and Polyester Ropes Used in Fall Arrest Equipment

**Carlos Arrieta,[1] Yingying Dong,[1] André Lan,[2] Toan Vu-Khanh[1]**

[1]Department of Mechanical Engineering, École de Technologie Supérieure, Montreal H3C 1K3, Canada

[2]Mechanical and Physical Risk Prevention - Research and Expertise Division, Institut de Recherche Robert-Sauvé en Santé et Sécurité du Travail, De Maisonneuve Ouest, Montreal H3A 3C2, Canada

*Correspondence to*: C. Arrieta (E-mail: carlos.arrieta.1@ens.etsmtl.ca).

**ABSTRACT:** In this work, the effect of natural climatic aging on two ropes made from polyamide 6 (PA6) and poly(ethylene terephthalate) (PET) was evaluated. Samples of rope from both materials underwent a continuous outdoor aging treatment spanning 6 months in Montreal's weather. Tensile tests carried out on aged PA6 ropes showed an increase in ultimate strain and a decrease in breaking force when compared with as-received values, while PET ropes exhibited a slight increase in ultimate strain as their breaking force remained unchanged. FTIR analyses of aged PET samples revealed a new absorption band in the hydroxyl region ascribed to the —OH stretching vibrations of carboxylic acid end groups. FTIR quantitative analyses of the absorption bands in the carbonyl region of aged PA6 spectra displayed an increase in intensity that indicates the occurrence of chemical degradation reactions. The degree of crystallinity of PA6, calculated from differential scanning calorimetry data, was found to increase after the weathering treatment, a result confirmed by X-ray diffraction analyses. The higher crystalline fraction is believed to entail an increase in the density of PA6 fibers, which give rise to the length reduction seen in PA6 ropes after the aging treatment. © 2013 Wiley Periodicals, Inc. J. Appl. Polym. Sci. 130: 3058–3065, 2013

**KEYWORDS:** aging; fibers; mechanical properties; X-ray

Received 8 March 2013; accepted 8 May 2013; Published online 8 June 2013

**DOI: 10.1002/app.39524**

## INTRODUCTION

Among the different synthetic fibers used in the manufacturing of fall arrest ropes and lifelines, polyamide and polyester fibers are the two most widely used. Owing to a combination of high tensile strength, good chemical resistance, and flexibility,[1] fall protection ropes made from these fibers offer a high-load-bearing capacity, which makes them an adequate choice when personal safety is considered. Both polymers, however, are known to be susceptible to chemical degradation caused by environmental agents such as light radiation and moisture.[2,3] Given that fall arrest ropes are intended for outdoor use (i.e., by construction or building maintenance workers) where they are exposed to the elements, performance loss is bound to occur after a given amount of time in service. Unfortunately, the extent of this loss in performance is usually unknown. The vagueness of the current criteria of withdrawal from service for these ropes (most suppliers recommend to replace the ropes after 5–10 years) underlines the urgent need to find a better indicator to monitor the natural aging process.

As a polymer synthesized by condensation, polyamide is likely to undergo chemical attack from water in the presence of moisture, as the amide bond is especially susceptible to both acid and base-catalyzed hydrolysis.[24–11] Photodegradation of aliphatic polyamides is characterized by the cleavage of the —N—C— bond at short light radiation wavelengths (254 nm) to produce amine and aldehyde groups.[12] Photochemical degradation of polyamides following exposure to light at wavelengths of 300 nm and higher (the solar spectral region) has been a topic of discussion as some authors report that because polyamides are unable to absorb radiation at wavelengths higher than 254 nm, light-induced aging effects are caused by chromophoric impurities,[2] while others claim that photodegradation in polyamide is the result of the direct photoscission of the amide bond.[11]

Poly(ethylene terephthalate) (PET), much like polyamide, is a condensation polymer prone to hydrolysis, catalyzed either by an alkali or an acid when exposed to humid environments due to the presence of the hydrolyzable ester group.[2,6,13–20] The hydrolysis of PET is particularly deleterious, given its autocatalytic nature (the increase in concentration of carboxyl end groups accelerates the rate of hydrolytic degradation).[2,16] The molecular weight decrease resulting from the hydrolysis reaction has a detrimental impact on the ultimate properties of the polymer such as tensile strength and ultimate elongation.[14,16,17,20]

© 2013 Wiley Periodicals, Inc.

**Table I.** Precipitation, Hours of Insolation, and Daily Average Irradiance by Month in Montreal

| Month | Amount of precipitation[a] (mm) | Numbers of hours of solar insolation[b] | Daily average value of solar irradiance ($kW/m^2$)[c] |
|---|---|---|---|
| December | 96.0 | 80.2 | 1.37 |
| January | 30.2 | 101.6 | 1.53 |
| February | 10.8 | 123.9 | 2.43 |
| March | 34.6 | 158.9 | 3.77 |
| April | 66.6 | 173.3 | 5.31 |
| May | 91.8 | 229.7 | 6.22 |

[a] Data taken from Pierre-Elliot Trudeau International Airport station. Only rain considered.[30b] Based on average historic data from the period 1971–2000.[30c] Average over 22-year period. Data taken from NASA Langley Research Centre.[31]

Photochemical aging of PET has been studied in several publications.[2,14–17,21–29] The main features displayed by PET upon UV irradiation in air at wavelengths between 300 and 420 are the decrease in tensile strength and ultimate elongation, the formation of carboxylic acid end groups, and the evolution of CO and $CO_2$ as volatiles.[2,21–23,26–29]

Although there is abundant literature regarding the photochemical and hydrolytic aging of polyamides and polyester, most of these studies are carried out in laboratory environments under controlled conditions and using accelerated aging treatments. Therefore, it is unknown whether the conclusions extracted from these studies can be translated to materials aged outdoors. The climatic weathering results will be compared to accelerated aging treatments carried out in laboratory. The goal of the present work is to characterize the degradation process of two types of rope (polyamide 6 and polyester) after 6 months of outdoor exposure in Montreal's (Canada) climate.

## EXPERIMENTAL

### Materials

The materials included in this study are two types of rope made from polyamide 6 (PA6) and PET fibers having a linear density of 147.36 and 178.62 kTex, respectively. Both ropes are 16 mm in diameter, and their construction consists of three braided strands. The ropes were provided by Barry Cordages (Montreal).

### Weathering Treatments

Spliced samples of PA6 and PET ropes ~180 cm long were attached in a vertical position to a wooden frame located on the rooftop of one of the buildings of École de technologie supérieure in Montreal (coordinates: 45°29'40"N, 73°33'45"W). No additional load was applied to the ropes, as they were allowed to hang freely under their weight between the fastening points in the frame. The rope samples were exposed to the outdoor elements for 6 months between December 9, 2011 and June 9, 2012. Relevant monthly weather data during this period are shown in Table I.

### Mechanical Properties

The breaking force and ultimate elongation of PA6 and PET ropes were measured according to Cordage Institute standard CI 1500 V.2 for uncycled breaking force.[32] Tensile tests were carried out at Barry Cordages facilities using a custom-built constant rate of extension tensile testing bench equipped with automated data collection software. After measuring their initial length, spliced specimens of rope were fastened to the crossheads of the bench and pulled apart at a speed of 100 mm/min. For both materials, the force versus elongation curve yielded by tensile tests displays several maxima associated with the failure of individual strands. The breaking force was defined as the force at the first maximum in the load versus elongation curve, which corresponds to the failure of a single strand. The reported breaking force value was taken as the average of five tests. Accordingly, ultimate elongation was taken as the average elongation at failure of the first strand to fail of five tests.

### Fourier Transform Infrared Analyses

FTIR spectra were collected with a Thermo Continu$\mu$m FTIR microscope in transmission mode using the KBr pellet method. Approximately 10 mg of material was dissolved in 10 mL of *m*-cresol at elevated temperature. When dissolving aged PA6 and PET, care was taken to select fibers located in the outer layers of the strands to ensure that the material had been actually exposed to the outdoor weather, as chemical degradation is believed to be confined to the surface of ropes at this stage of the aging process. Once complete dissolution was achieved, a mixture of the solution (~5 mL) with spectroscopic quality KBr powder (~25 mg) was prepared. Excess solvent was removed through evaporation, after which the pellet was made using a manual press. A total of 128 scans at 8 $cm^{-1}$ resolution were collected to produce each spectrum. The average absorbance value of five measurements was used for quantitative analysis. The height of absorbance bands was used to evaluate spectral data of PET fibers, whereas the area of absorbance bands was chosen instead for the analysis of PA6 results. No subtraction of the solvent spectrum was done, because no absorption bands corresponding to *m*-cresol were detected in the final spectrum.

### Differential Scanning Calorimetry Analyses

Differential scanning calorimetry (DSC) analyses were conducted using a Pyris 1 Perkin Elmer calorimeter. Samples weighing 5–10 mg were heated from −10 to 300°C at a rate of 10°C/min. Material crystallinity was calculated using Eq. (1).

$$X_{cr} = \frac{H_{ms}}{H_{m0}} \quad (1)$$

where $X_{cr}$ is the crystalline fraction of the material and $H_{ms}$ and $H_{mo}$ are the enthalpies of fusion of the sample and the entirely crystalline material, respectively.

### X-Ray Diffraction Analyses

X-ray diffraction profiles of PA6 fibers were obtained using Ni-filtered Cu K$\alpha$ X-ray radiation in a Pananalytical X'Pert Pro diffractometer operating at a voltage of 45 kV and a current of 40 mA. The $2\theta$ range selected for the diffractograms was 5°–30°C. The profiles were corrected for air scatter, polarization, Compton scatter, and Lorentz effect.

## RESULTS

### Mechanical Properties

Before tensile testing, length measurements and visual inspection of individual specimens of rope were performed to detect

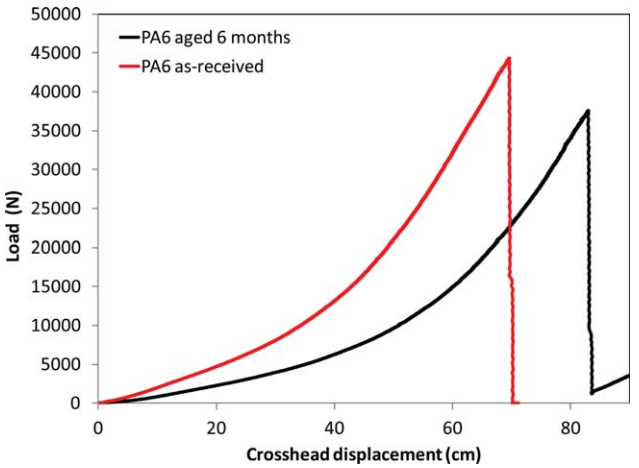


**Figure 1.** Comparison of a typical load versus crosshead-displacement curve for as received and aged PA6 ropes. [Color figure can be viewed in the online issue, which is available at wileyonlinelibrary.com.]

changes in color and length induced by the outdoor weathering treatment. Although no significant changes in the color of aged specimens were found when compared with as-received ones, a noticeable decrease of about 6% (~13 cm) in the length of aged PA6 ropes was observed. The length of aged PET ropes, on the other hand, remained constant throughout the aging treatment.

The typical aspect of the load versus crosshead-displacement curve for PA6 and PET ropes in as-received and aged conditions is shown in Figures 1 and 2, respectively.

From Figure 1, it is readily seen that the impact of the weathering treatment on the mechanical properties of PA6 ropes is reflected by a small decrease of the tensile breaking force as well as a significant increase in the elongation at break. Although the decrease of the tensile load of PA6 after outdoor exposure is in good agreement with the general depiction of the mechanical behavior of polymers undergoing chemical degradation[2,3,14] and might be explained by the occurrence of a chain scission process initiated by either the photolysis or the hydrolysis of the polyamide molecules, as suggested by the results of the FTIR

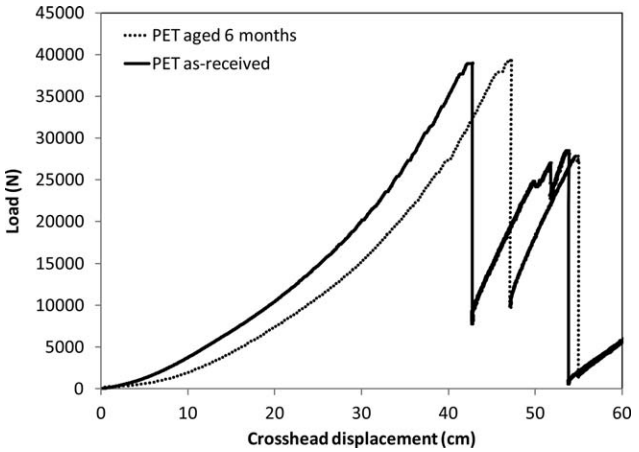


**Figure 2.** Comparison of a typical load versus crosshead-displacement curve for as-received and aged PET ropes.

analyses of PA6 fibers after the weathering treatment (see the FTIR analyses section below), the increase of the elongation at break of aged ropes is an unexpected outcome, because ultimate properties are expected to deteriorate following chemical degradation.[3] PET ropes on the other hand, while displaying a slight increase in ultimate elongation as well, are seemingly less affected by environmental aging factors than PA6 ropes, as their breaking force remained essentially constant after the weathering treatments.

The summary of the results of the tensile tests is shown in Table II. As expected, the ultimate strain of aged PA6 ropes (which accounts for both the increase in crosshead-displacement and the decrease in specimen length) shows an important increase (~30%) compared to as-received ones.

### Fourier Transform Infrared Analyses

The qualitative analysis of the hydroxyl region (3200–3500 $cm^{-1}$) of PET spectra revealed the formation of a new absorption band toward 3300 $cm^{-1}$ following the aging treatment. This band has been tentatively ascribed to the —OH stretching vibration of newly formed carboxylic acid end groups, which are believed to be the product of chemical degradation reactions resulting from outdoor exposure. The development of this band is consistent with previous works on the chemical degradation of PET.[23,28] A comparison of the spectra of as-received and aged PET fibers in the 2700–3500 $cm^{-1}$ region is shown in Figure 3.

During PET degradation, carboxylic acid end groups are the final product of either an acid-catalyzed hydrolysis (along with hydroxyl groups) or a photooxidation reaction that follows a Norrish type I or II chain-scission process (see Figure 4). Consequently, the formation of the absorption band at 3300 $cm^{-1}$ provides evidence that PET ropes have undergone a chemical degradation process during the outdoor exposure treatment. Although a quantitative analysis of the bands corresponding to the hydroxyl groups would allow estimating the relative contribution of photochemical and hydrolytic aging reactions in the evolution of COOH end groups, the bands associated with the hydroxyl groups are believed to overlap the existing bands in the spectrum of PET, which hinders the tracing of the origin of the carboxylic acid species evolved during the weathering treatment.

The concentration of carboxylic acid species can be calculated using Beer–Lambert's law:

$$A_\lambda = \varepsilon_{COOH(\lambda)} l C_{COOH} \Rightarrow C_{COOH} = \frac{A_\lambda}{\varepsilon_{COOH(\lambda)} l} \qquad (2)$$

where $A_\lambda$ is the absorbance value at wavelength $\lambda$, $\varepsilon_{COOH(\lambda)}$ is the molar absorption coefficient of carboxylic acid species at wavelength $\lambda$, $l$ is the optical path of the infrared radiation (the thickness of the pellet), and $C_{COOH}$ is the concentration of carboxylic acid. $C_{COOH}$ was taken as the average of five solutions of eq. (2) using different sets of data. Taking the value of $\varepsilon_{COOh(3300)} = 150M^{-1}$ $cm^{-1}$ reported by Day and Wiles[23] gives a value of $C_{COOH} = 4.706 \times 10^{-3}M$. It is worthwhile noticing that this calculated concentration of carboxylic acid species concerns only the fibers located on the surface of the strands of PET, because the progress of the reaction in the bulk of the

**Table II.** Summary of Tensile Testing Results

| Type of rope | Condition | Tensile breaking force (kN) | | Ultimate strain (mm/mm) | | Residual tensile breaking force[a] (%) | Residual Ultimate strain[a] (%) |
|---|---|---|---|---|---|---|---|
| PA6 | As-received | Mean | 41.96 | Mean | 0.389 | 91.55 | 128.8 |
| | | Std. dev. | 2.05 | Std. dev. | $8.94 \times 10^{-3}$ | | |
| | Aged 6 months | Mean | 38.41 | Mean | 0.501 | | |
| | | Std. dev. | 0.62 | Std. dev. | $2.94 \times 10^{-3}$ | | |
| PET | As-received | Mean | 38.53 | Mean | 0.247 | 102.58 | 110.5 |
| | | Std. dev. | 0.95 | Std. dev. | $5.44 \times 10^{-3}$ | | |
| | Aged 6 months | Mean | 39.41 | Mean | 0.273 | | |
| | | Std. dev. | 2.84 | Std. dev. | $1.87 \times 10^{-2}$ | | |

[a] Residual property is calculated as the ratio aged value/as-received value.

ropes is expected to be affected by other parameters, such as the availability of oxygen and water in the inner layers of the strands, which were not considered in the calculation.

No new absorption bands were observed to develop in the FTIR spectrum of PA6 after the outdoor exposure. Photodegradation of PA6 is expected to result in the formation of aldehydic and acidic groups, whereas carboxylic acid and amine groups are the final products of the hydrolysis reaction.[24–11] Both aldehydes and acid groups display a strong absorption band in the carbonyl region (1650–1800 $cm^{-1}$) corresponding to the C═O stretching vibration that makes IR band assignment a relatively straightforward procedure. The FTIR spectrum of as-received PA6, however, already exhibits strong bands in the carbonyl region, and so any new band in this region linked to the formation of chemical degradation products is bound to overlap the existing bands. A careful inspection of the spectrum of aged PA6 fibers, however, reveals a slight increase in the intensity of the bands in the 1700–1800 $cm^{-1}$ region, as seen in Figure 5.

Given the difficulty entailed by the overlapping of absorption bands when assigning individual bands to specific degradation products, the area of the absorption bands in the carbonyl region was chosen over the height of individual bands as the parameter to quantify the spectra of aged PA6 fibers. The method used for quantitative analysis consisted in calculating the ratio $I_{carbonyl}/I_{1465\ cm^{-1}}$ by normalizing the area of the group of bands in the 1700–1800 $cm^{-1}$ region using the area of the band at 1465 $cm^{-1}$ (ascribed to the bending vibration of $CH_2$ molecules) as reference (see Figure 6).

The $I_{carbonyl}/I_{1465\ cm^{-1}}$ ratio, calculated as the average of five different analyses, was found to go from 0.589 to 0.683, which corresponds to ~16% increase in intensity. This increase suggests the formation of photooxidation (aldehyde or carboxylic acids) products or carboxylic acids resulting from hydrolysis reactions, which exhibit all an absorption band in the carbonyl region. As with PET fibers, the absorption bands corresponding to amine end groups, which may be used to estimate the amount of

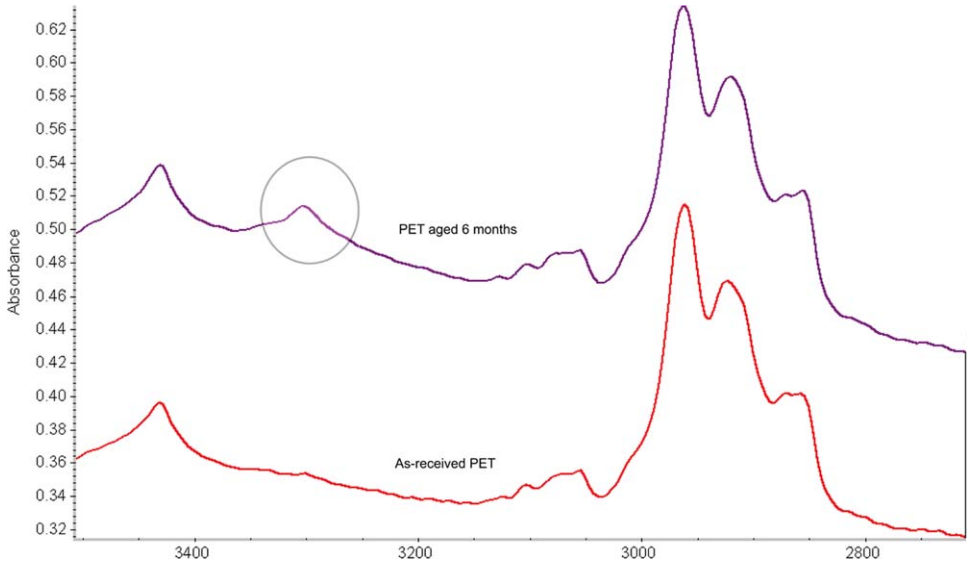


**Figure 3.** Spectra of as-received and aged PET fibers. The band corresponding to newly formed carboxylic acid end groups is encircled. [Color figure can be viewed in the online issue, which is available at wileyonlinelibrary.com.]

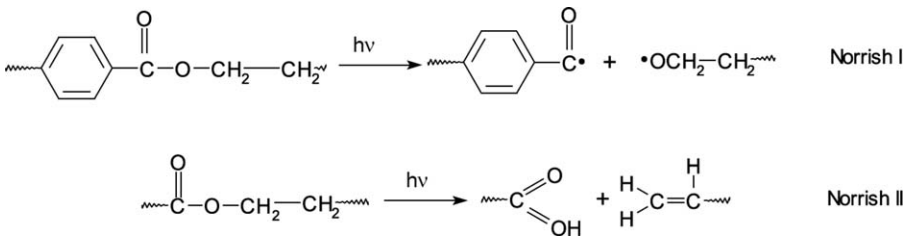


**Figure 4.** Norrish type I and II chain scission processes.

carboxylic acid end groups produced by hydrolysis, were not discernible in the spectrum of aged PA6.

### Melting Behavior and Material Crystallinity

The crystalline fraction of PA6 and PET was calculated using eq. (1) with $H_{m0}$ taken as 117[26] and 240[33] J $g^{-1}$ for PET and PA6, respectively. The thermograms of as-received and weathered PA6 and PET fibers are shown in Figures 7 and 8, respectively. The crystalline fraction for as-received PA6 was found to increase from 16 to 33% after the weathering treatment, indicating a twofold increment in crystallinity. X-ray diffraction analyses were carried out to confirm these results. The diffraction profile of PA6 fibers before and after the weathering treatment is shown in Figure 9. The two crystalline peaks characteristic of the $\alpha$ phase can be observed in the diffractogram of the as-received PA6 fiber at 20.5° and 23.2°. These two peaks correspond to the 200 and 002/202 reflections, respectively.[34] The diffraction profile of PA6 fibers after a 6-month weathering treatment revealed an increment of the size of the two peaks in the crystalline phase, indicating an increase of the crystalline fraction of the material. The full width at half maximum, a parameter associated with the size and perfection of crystals, increases as well for both peaks, suggesting that the aging treatment leads to crystallites of larger dimensions. A similar result has been reported by Murthy et al.[35] after exposing nylon 6 fibers to high humidity at room temperature. The authors argue that in the presence of moisture, PA6 molecules in the crystalline $\gamma$ phase and the amorphous region gain in mobility and are able to migrate toward the lower-energy-conformation $\alpha$ phase. This hypothesis may hold as well in the case of the current weathering treatment with an additional consideration, namely that, as suggested by the FTIR analyses, the weathering treatment may result in a chain scission process that reduces the length of PA6 molecules, increasing their mobility even further.

Two features can be readily noticed in the thermogram of weathered PET fibers in Figure 8: a broadening of the melting endotherm and a shift of the onset of the melting peak toward lower temperatures. These results suggest that as the weathering treatment proceeds, the crystallites in the as-received PET fibers break down into smaller crystals having lower melting temperatures. The breaking down of larger PET crystallites into smaller ones leads to a larger spectrum of crystallite sizes that display a wider range of melting temperatures, hence the broader melting peak seen in the thermogram of PET.

The outdoor exposure of PA6 and PET ropes leads to opposite results regarding the crystalline fraction of both polymers, as it decreases in the case of PET while it increases for PA6.

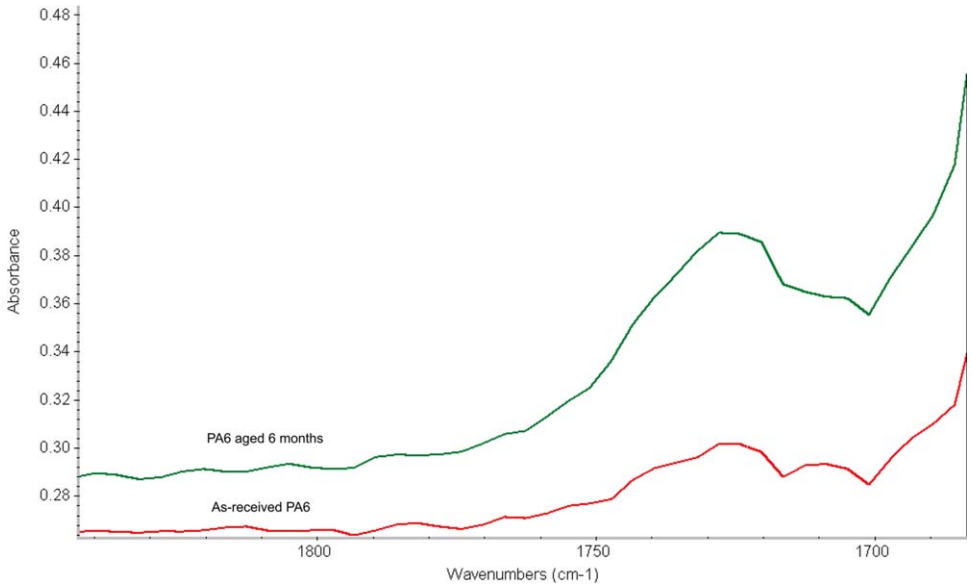


**Figure 5.** Comparison of the spectra of as-received and aged PA6 in the 1700–1800 $cm^{-1}$ region. [Color figure can be viewed in the online issue, which is available at wileyonlinelibrary.com.]

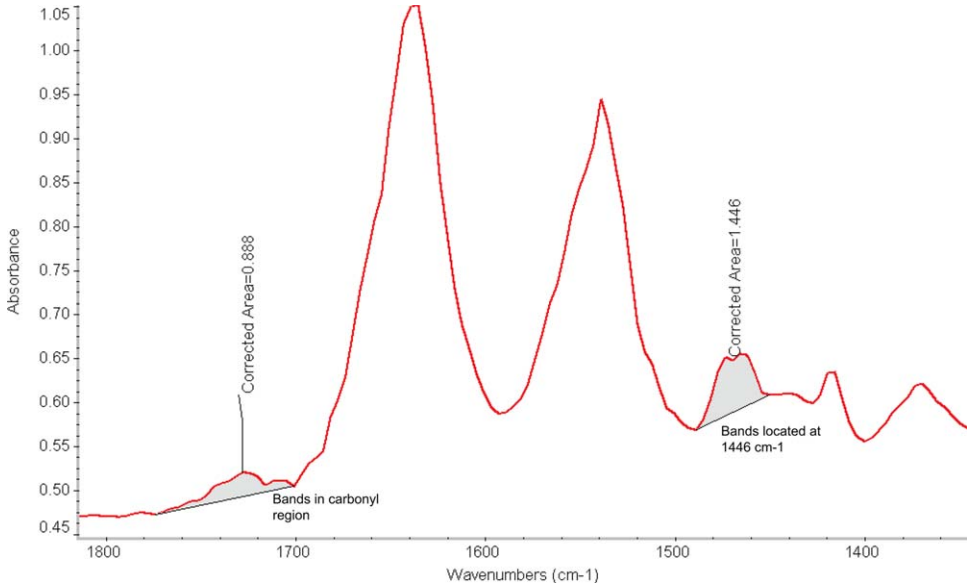


**Figure 6.** Illustration of the procedure used for analysis of the spectra of aged PA6 fibers. [Color figure can be viewed in the online issue, which is available at wileyonlinelibrary.com.]

## DISCUSSION

Although the results presented in the previous section seem to suggest that both chemical degradation (in the form of photoxidation and/or hydrolysis reactions) and physical aging (recrystallization) take place during the outdoor exposure of the ropes, it is still unclear how these two processes relate to the unexpected phenomena observed in PA6 after the weathering treatments, namely the length reduction and the increase of the ultimate strain. An understanding of the mechanisms underlying these baffling observations is needed to gain a deeper insight into the weathering process of this material. Assuming that the mass of the ropes remains constant throughout the weathering treatment, a higher density brought about by the larger crystalline fraction found in aged PA6 fibers would be the most likely phenomenon to account for the significant reduction in the length of PA6 ropes observed after aging. The larger crystalline phase entails an increase of the density of the material, as the molecules in the less ordered amorphous and crystalline $\gamma$ phases arrange themselves in the more closely packaged manner characteristic of the $\alpha$ phase. Because the mass of the fiber remains constant, the volume of the fiber needs to be reduced accordingly, prompting the decrease in length seen in aged PA6 ropes.

The other observation that opposes the normal depiction of aged materials is the enhancement of the ultimate strain of weathered PA6. As mentioned earlier, weathering treatments are expected to worsen the mechanical properties of polymers, which in the case of ultimate strain normally translates into a decrease of the property. The increase of crystallinity of treated PA6 fibers may be once again the underlying phenomenon causing the increase in ultimate strain. Although different properties are assigned to the PA6 fiber as a whole, the amorphous and crystalline phases within a fiber exhibit different properties when a mechanical load is applied, including a different elastic

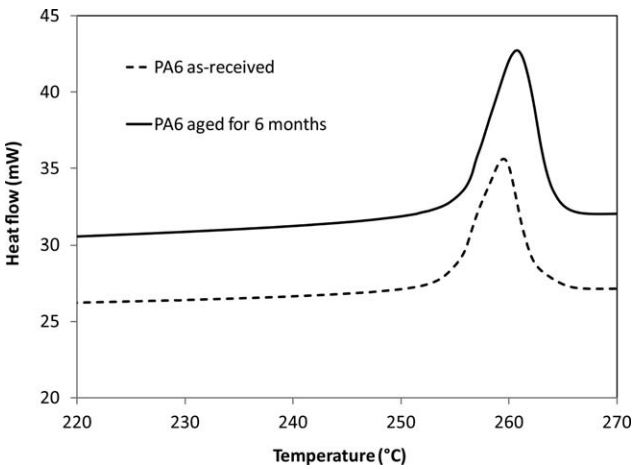


**Figure 7.** DSC thermograms of as-received and weathered PA6 fibers.

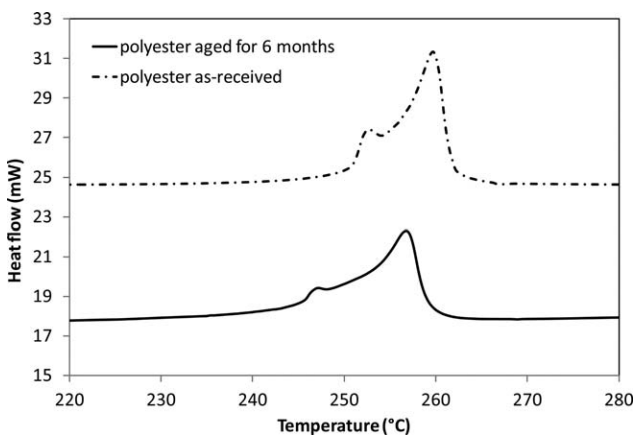


**Figure 8.** DSC thermograms of as-received and weathered PET fibers.

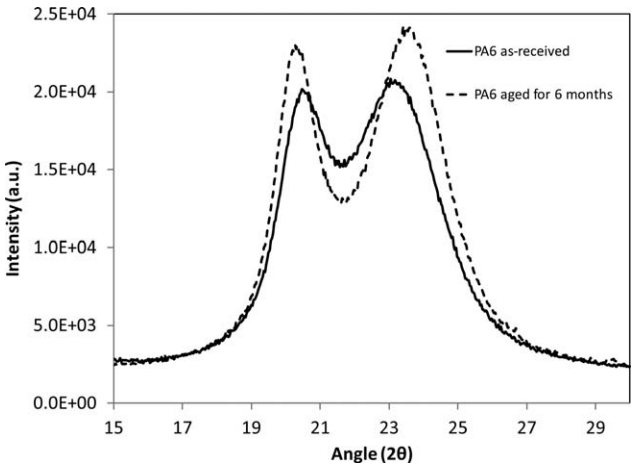


**Figure 9.** XRD profile of as-received and aged PA6 fibers.

modulus. The strength of the fiber is believed to be controlled by the presence of defects in its structure, whereas the elastic modulus of PA6 fibers as an aggregate of the amorphous and crystalline regions (microfibrils) is governed by the joint behavior of the microfibrils that support the load and the extended molecules between microfibrils, which transmit the force among them.[36,37] As the crystallinity of PA6 increases with the weathering treatment, a larger fraction of the load applied during tensile tests is supported by microfibrils, which have a higher elastic modulus, and thus yield a smaller strain than nonaged samples when subjected to a similar level of stress. The overall tensile strain in the PA6 rope is consequently reduced, so that when the failure stress is reached, the extent of the deformation is larger than in the case of the as-received sample, which has a lower crystalline fraction.

At this stage of the outdoor weathering program we have undertaken, most of the processes responsible for the changes in mechanical properties are believed to be physical in nature. This is highlighted by the fact that PET rope, which exhibits solid indications of undergoing chemical degradation reactions after outdoor exposure, is the least affected by the weathering treatment in terms of loss of mechanical performance out of the two materials included in this study.

## CONCLUSIONS

Samples of rope made from PA6 and PET fibers were exposed for 6 months to the outdoor weather of Montreal. The length of PA6 ropes was found to decrease after the aging treatment while the length of PET ropes remained constant. Tensile tests carried out on weathered PA6 ropes revealed that the outdoor exposure resulted in a slight decrease in tensile breaking force and a significant increase of ultimate strain. The tensile breaking force of aged PET ropes remained virtually constant while their ultimate strain showed a little increase. FTIR spectra of aged PET fibers revealed the formation of a new absorption band toward 3300 $cm^{-1}$. This band was ascribed to carboxylic acid end groups, which are believed to be the product of either photochemical or hydrolytic degradation reactions. The intensity of the bands in the carbonyl region of FTIR spectra of aged PA6 fibers increased after outdoor exposure, a result that suggests that PA6 fibers have undergone chemical degradation reactions. The crystallinity of PA6 fibers, calculated from DSC data, was found to undergo a twofold increase after the weathering treatment, a result bolstered by the increase of the intensity of the peaks associated to the crystalline phase in the XRD profile of aged PA6 fibers. The increase in density caused by the larger crystalline phase seems to be the underlying phenomenon causing the decrease in length observed in aged PA6 ropes.

The significant increase in ultimate strain of weathered PA6 ropes is likely related to an increase in the elastic modulus of the PA6 fibers caused by the augmentation of the crystalline phase.

## ACKNOWLEDGMENTS

The authors thank the staff of Barry Cordages, especially Mr. Benoit Thibert and Mrs. Liseth Figueroa, for their kind assistance during the mechanical tests carried out in their facilities.

## REFERENCES

1. Vasanthan, N. In Handbook of Textile Fibre Structure; Eichhorn, S. J., Hearle, J. W. S., Jaffe M., Kikutani, T., Eds.; Woodhead: Cambridge, **2009**; Vol. *1*, Chapter 7, p 232–256.
2. Carlsson, D. J.; Wiles, D. M. In Encyclopedia of Polymers Science and Engineering; Francis, M. H., Ed.; Wiley: New York, **1985**; Vol. *4*, "Degradation," p 630–697.
3. Verdu, J. In Techniques de l'Ingénieur, Traité Plastiques et Composites, Edn T.I.; AM 3 151, Vieillissement Chimique des Plastiques: Aspects Généraux, **2002**; p 1–14.
4. Bernstein, R.; Derzon, D. K.; Gillen, K. *Polym. Degrad. Stab.* **2005**, *88*, 480.
5. Cribbs, D.; Ogale, A. A. *Text. Res. J.* **2003**, *73*, 98.
6. Sudduth, R. *Polym. Eng. Sci.* **1996**, *36*, 2135.
7. Meyer, A.; Jones, N.; Lin, Y.; Kranbuehl, D. *Macromolecules* **2002**, *35*, 2784.
8. Jacques, B.; Werth, M.; Merdas, I.; Thominette, F.; Verdu, J. *Polymer* **2002**, *43*, 6439.
9. Mohd Ishak, Z. A., Berry, J. P. *J. Appl. Polym. Sci.* **1994**, *51*, 2145.
10. Wu, C.; Mantell, S. C.; Davidson, J. *J. Sol. Energy Eng.* **2004**, *126*, 581.
11. Thominette, F.; Merdas, I.; Verdu, J. In Proceedings of the 21st International Conference on Offshore Mechanics and Arctic Engineering, Oslo, Norway, June 22–28, 2002, American Society of Mechanical Engineers, **2002**.
12. Lemaire, J.; Gardette, J. L.; Rivaton, A.; Roger, A. *Polym. Degrad. Stab.* **1986**, *15*, 1.
13. Hunter, L. J.; White, W.; Cohen, P. H.; Biermann, P. *J. John Hopkins Appl. Tech. Dig.* **2000**, *21*, 575.
14. Duvall, D. E. *Polym.-Plast. Technol. Eng.* **1995**, *34*, 227.
15. Edge, M.; Hayes, M.; Mohammadian, M.; Allen, N. S.; Jewitt, T. S.; Brems, K.; Jones, K. *Polym. Degrad. Stab.* **1991**, *32*, 131.

16. Allen, N. S.; Edge, M.; Mohammadian, M.; Jones, K. Physicochemical aspects of the environmental degradation of poly(ethylene terephthalate). *Polym. Degrad. Stab.* **1994**, *43*, 229.
17. Allen, N. S.; Edge, M.; Mohammadian, M.; Jones, K. *Eur. Polym. J.* **1991**, *27*, 1373.
18. Sammon, C.; Yarwood, J.; Everall, N. *Polym. Degrad. Stab.* **2000**, *67*, 149.
19. Ganem, M.; Mortaigne, B.; Bellenger, V.; Verdu, J. *Polym. Networks Blends* **1994**, *4*, 87.
20. Chen, Y.; Ding, X.; Li, Y. *Fibers Polym.* **2012**, *13*, 169.
21. Day, M.; Wiles, D. M. *J. Appl. Polym. Sci.* **1972**, *16*, 175.
22. Day, M.; Wiles, D. M. *J. Appl. Polym. Sci.* **1972**, *16*, 191.
23. Day, M.; Wiles, D. M. *J. Appl. Polym. Sci.* **1972**, *16*, 203.
24. Allen, N. S.; Edge, M.; Mohammadian, M.; Jones, K. *Polym Degrad. Stab.* **1993**, *41*, 191.
25. Sasamoto, T.; Desai, P.; Abhiraman, A. S. *Polym. Mater.* **1992**, *67*, 393.
26. Fechine, G. J. M.; Souto-Maior, R. M.; Rabello, M. S. *J. Mater. Sci.* **2002**, *37*, 4979.
27. Fechine, G. J. M.; Christensen, P. A.; Egerton, T. A.; White, J. R. *Polym. Degrad. Stab.* **2009**, *94*, 234.
28. Grosstête, T.; Rivaton, A.; Gardette, J. L.; Hoyle, C. E.; Ziemer, M.; Fagerburg, D. R.; Clauberg, H. *Polymer* **2000**, *41*, 3541.
29. Hurley, C. R.; Leggett, G. J. *ACS Appl. Mater. Interf.* **2009**, *1*, 1688.
30. Environment Canada. www.climate.weatheroffice.gc.ca. (accessed August 22, 2012).
31. NASA Langley atmospheric science data center. http://eos-web.larc.nasa.gov (accessed August 22, 2012).
32. Cordage Institute International Standard CI 1500 V.2. 2006. Tests Methods for Fiber Rope. Cordage Institute, Wayne PA, 17 p.
33. Fornes, T. D.; Paul, D. R. *Polymer* **2003**, *44*, 3945.
34. Ramesh, C.; Bhoje Gowd, E. *Macromolecules* **2001**, *34*, 3308.
35. Murthy, N. S.; Aharoni, S. M.; Szollosi, A. B. *Polym. Sci., Part A-2: Polym. Phys.* **1985**, *23*, 2549.
36. Peterlin, A. *Polym. Eng. Sci.* **1977**, *18*, 1062.
37. George, G. A. *Mater. Forum* **1995**, *19*, 145.